SLAC–PUB–9788
August 2003

Impact of beam energy modulation on rf zero-phasing microbunch measurements*

Z. Huang
Stanford Linear Accelerator Center, Stanford, CA 94309

T. Shaftan
Brookhaven National Laboratory, Upton, NY 11973

Abstract

Temporal profile of a simple bunch distribution may be obtained by measuring the horizontal density profile of an energy-chirped electron beam at a dispersive region using the rf zero-phasing technique. For an energy-modulated beam, the horizontal profile obtained by this technique is also modulated with an enhanced amplitude. We study the microbunching experiment at the NSLS source development laboratory and show that the horizontal modulation observed by the rf zero-phasing technique can be explained by the space-charge induced energy modulation in the accelerator.

*Work supported by Department of Energy contracts DE–AC03–76SF00515 and DE–AC02–76CH00016.

1 Introduction

Time-resolved measurements of very short electron bunches are essential for free-electron lasers (FEL), linear colliders and other advanced accelerators. Diagnostic techniques that have femtosecond resolutions are of particular interests (see, e.g., Ref. [1]). Among them, the rf-zero phasing technique [2] is relatively straightforward to implement since accelerating cavities and regions of nonzero dispersion are usually available at linear accelerators. Knowledge of the horizontal density profile at the dispersive region determines the energy profile of the bunch, which in turn can be related to the current profile for a linearly-chirped beam. Recent applications of such a technique at the NSLS source development laboratory (SDL) yield unexpected information about the longitudinal bunch distribution [3]: the measured horizontal density profiles show large high-frequency modulations after the beam is compressed by a bunch compressor chicane. Analysis based on the recently developed coherent synchrotron radiation (CSR) instability in the bunch compressor [4, 5] does not yield microbunching that supports the observed structures [6]. Note that similar structures in energy spectra of chirped electron beams due to off-crest rf acceleration have been reported in Ref. [7, 8, 9].

Motivated by these experimental observations, we perform a thorough analysis of the rf zero-phasing technique for a general beam distribution. We show that the horizontal density modulation obtained by this method is significantly enhanced due to the beam energy modulation. For the SDL experiment, the energy modulation can be induced by the longitudinal space charge (LSC) force in the linac and can dominate the horizontal spectrum. Thus, the rf zero-phasing technique may be used to measure the beam energy modulation, which plays a major role in the microbunching instability driven by various impedance elements in accelerators for future x-ray FELs [10, 11, 12].

2 Analysis of rf zero-phasing technique

The rf zero-phasing technique uses one or several rf cavities operated at the zero accelerating phase to impart a large energy-time correlation to the beam. The energy-chirped beam is then dispersed horizontally by a spectrometer dipole and intercepted by a measurement screen. The horizontal profile of the beam at the screen is used to determine its energy profile, which can be related to its temporal profile for a beam with a smooth, linear energy-time phase space distribution (see Fig. 1).

In general, we consider a distribution function $f(x, x', z, \delta; s)$ in a dispersive region at a distance s from the beginning of the spectrometer dipole. Here x and $x' \equiv dx/ds$ are the horizontal phase space coordinates, z is the longitudinal (temporal) coordinate centered in the bunch ($z > 0$ for the head of the bunch), and $\delta = \Delta E/E_0$ is the relative energy deviation for a beam with the average energy $E_0 = \gamma mc^2$. The horizontal beam density profile at s is

$$F(x; s) = \int dx' dz d\delta f(\mathbf{X}; s)\,, \tag{1}$$

where we use the shorthanded notation $\mathbf{X} = (x, x', z, \delta)$ and take the normalization $\int d\mathbf{X} f(\mathbf{X}; s) =$

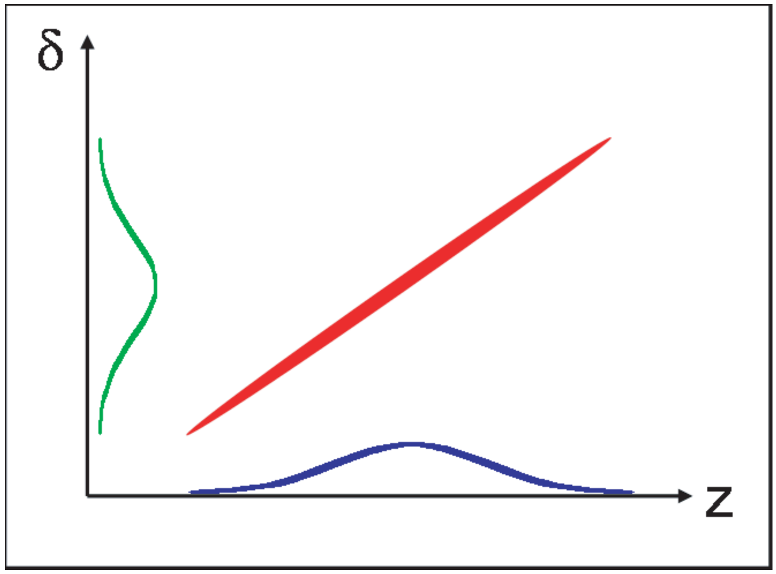

Figure 1: (Color) Current profile (in blue) and energy profile (in green) for a beam with a smooth, linear energy-time ($\delta - z$) phase space distribution (in red).

N to be the total number of electrons. Making a Fourier transformation in x, we have

$$\begin{aligned} a(k_\mathrm{m}; s) =& \frac{1}{N}\int dx e^{-ik_\mathrm{m}x} F(x; s) = \frac{1}{N}\int d\mathbf{X} e^{-ik_\mathrm{m}x} f(\mathbf{X}; s) \\ =& \frac{1}{N}\int d\mathbf{X}_\mathrm{d} e^{-ik_\mathrm{m}x(\mathbf{X}_\mathrm{d})} f_d(\mathbf{X}_\mathrm{d}) , \end{aligned} \tag{2}$$

where k_m is the measured modulation wavenumber, $f_\mathrm{d}(\mathbf{X}_\mathrm{d})$ is the beam distribution at the entrance of the dipole (referred to by the subscript d), and we have applied the Liouville theorem in transforming the phase space from s to the beginning of the dipole [13].

Let us assume that the beam at the entrance of the dipole has both a small longitudinal density variation $\Delta n(z_\mathrm{d})$ as well as a small energy variation $\Delta\delta(z_\mathrm{d})$, i.e.,

$$f_\mathrm{d}(\mathbf{X}_\mathrm{d}) = \frac{n_0 + \Delta n}{2\pi\varepsilon_x\sqrt{2\pi}\sigma_\delta} \exp\left[-\frac{x_\mathrm{d}^2 + (\beta_\mathrm{d}x'_\mathrm{d} + \alpha_\mathrm{d}x_\mathrm{d})^2}{2(\sigma_x)_\mathrm{d}^2} - \frac{(\delta_\mathrm{d} - hz_\mathrm{d} - \Delta\delta)^2}{2\sigma_\delta^2}\right] . \tag{3}$$

where n_0 is the average line density, ε_x is the horizontal emittance, σ_δ is the rms incoherent energy spread, α_d and β_d are the twiss parameters, $(\sigma_x)_\mathrm{d} = \sqrt{\varepsilon_x\beta_\mathrm{d}}$ is the rms horizontal beam size, and

$$h = \frac{eV_\mathrm{rf}k_\mathrm{rf}\cos\phi}{E_0} \tag{4}$$

is the energy chirp generated by an accelerating voltage V_rf with the rf wavelength $\lambda_\mathrm{rf} = 2\pi/k_\mathrm{rf}$ at a phase ϕ ($\phi = 0$ or π for zero-crossing). Note that the horizontal position x at s is

$$x(\mathbf{X}_\mathrm{d}) = C(s)x_\mathrm{d} + S(s)x'_\mathrm{d} + \eta(s)\delta_\mathrm{d} , \tag{5}$$

where $C(s), S(s), \eta(s)$ are the cosine-, sine-like and dispersion functions, respectively. Inserting Eq. (5) into Eq. (2) and keeping only first order terms in Δn and $\Delta\delta$, we obtain

$$\begin{aligned} a(k_{\mathrm{m}};s) &= [b_{\mathrm{d}}(k_{\mathrm{m}}\eta h) - ik_{\mathrm{m}}\eta p_{\mathrm{d}}(k_{\mathrm{m}}\eta h)] \\ &\qquad \times \exp\left[-\frac{k_{\mathrm{m}}^2\eta^2\sigma_\delta^2}{2} - \frac{k_{\mathrm{m}}^2(\sigma_x)_{\mathrm{d}}^2}{2}\left(\left(C - \frac{\alpha_{\mathrm{d}}S}{\beta_{\mathrm{d}}}\right)^2 + \frac{S^2}{\beta_{\mathrm{d}}^2}\right)\right] \\ &= \left[b_{\mathrm{d}}(k) - i\frac{k}{h}p_{\mathrm{d}}(k)\right]\exp\left[-\frac{k^2\sigma_\delta^2}{2h^2} - \frac{k^2\sigma_x^2(s)}{2\eta^2h^2}\right], \end{aligned} \tag{6}$$

where $k = k_{\mathrm{m}}(s)\eta(s)h$ is the initial modulation wavenumber, $b_{\mathrm{d}}(k)$ is the longitudinal bunching spectrum at the beginning of the dipole

$$b_{\mathrm{d}}(k) = \frac{1}{N}\int d\mathbf{X}_d f(\mathbf{X}_{\mathrm{d}})e^{-ikz_{\mathrm{d}}} = \frac{1}{N}\int dz_{\mathrm{d}}\Delta n(z_{\mathrm{d}})e^{-ikz_{\mathrm{d}}}, \tag{7}$$

$p_{\mathrm{d}}(k)$ is the energy spectrum at the beginning of the dipole

$$p_{\mathrm{d}}(k) = \frac{1}{N}\int d\mathbf{X}_d f(\mathbf{X}_{\mathrm{d}})\delta_d e^{-ikz_{\mathrm{d}}} = \frac{1}{N}\int dz_{\mathrm{d}}\Delta\delta(z_{\mathrm{d}})e^{-ikz_{\mathrm{d}}}, \tag{8}$$

and $\sigma_x(s)$ is the rms horizontal beam size at s. Note that Eq. (6) is valid when $|b_{\mathrm{d}}(k)| \ll 1$ and $|p_{\mathrm{d}}(k)| \ll h/k$. In the absence of any initial energy modulation (i.e., when the longitudinal phase space correlation is linear), and if

$$\lambda = \frac{2\pi}{k} \gg \max\left(\frac{\sigma_\delta}{|h|}, \frac{\sigma_x(s)}{\eta|h|}\right), \tag{9}$$

then

$$a[k_{\mathrm{m}}(s);s] \approx b_d(k)\,, \quad F(x;s) \approx \Delta n\left(\frac{x}{\eta(s)h}\right) \tag{10}$$

reproduces the longitudinal density variation (i.e., the current profile) at the entrance of the dipole. The right hand side of Eq. (9) determines the temporal resolution of the rf zero-phasing technique due to finite beam size and energy spread. For a high-brightness electron beam generated from a photocathode rf gun, the incoherent energy spread σ_δ is typically very small, and the horizontal beam size σ_x can be focused down to 100 μm or less at the measurement screen. If we take $|h| \approx 20$ m^{-1} and $\eta \approx 1$ m, Eq. (9) indicates a temporal resolution of about 5 μm or 17 fs.

However, if the longitudinal phase space distribution has a higher-order correlation, e.g., if the beam energy is modulated at a modulation wavelength λ, the energy modulation can be converted into horizontal density modulation through the dispersion and hence distort the simple relation given by Eq. (10). From Eq. (6), we see that the amplitude of the horizontal modulation is magnified by a factor

$$\frac{k}{|h|} = \frac{E_0}{eV_{\mathrm{rf}}|\cos\phi|}\frac{\lambda_{\mathrm{rf}}}{\lambda} \gg 1 \tag{11}$$

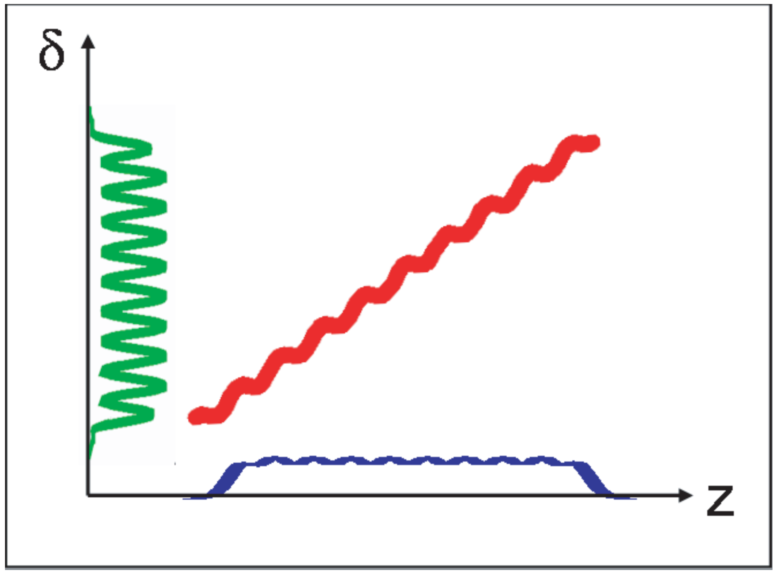

Figure 2: (Color) Current profile (in blue) and energy profile (in green) for a chirped beam with a modulated longitudinal phase space distribution (in red).

for $\lambda_{\rm rf} \gg \lambda$ above the resolution limit, even if $eV_{\rm rf} \approx E_0$ (i.e., 100% correlated energy spread). As illustrated in Fig. 2, the very rapid but small energy modulation on top of a linear chirp redistributes the electrons in the energy space, causing a very large density modulation in the energy spectrum.

Therefore, the horizontal (or energy) profile obtained by the rf zero-phasing technique is sensitive to even very small high-frequency energy modulation of the beam. For a current-modulated bunch, the energy modulation can be induced by wakefields in the accelerator. An important source of energy modulation for a high-brightness electron beam is the longitudinal space charge force in the linac. We study its effect on rf zero-phasing measurements in the next two sections.

3 Energy modulation due to space charge

There is no longitudinal space charge (LSC) force if the bunch current profile is uniform. However, if there is a density clustering, the longitudinal space charge force tends to push electrons away from each other, accelerating the front electrons and decelerating the back electrons to give rise to the energy modulation. For a sinusoidal current modulation at the modulation wavelength λ characterized by the bunching parameter $b(k)$, the longitudinal electric field in the absence of vacuum chamber is [14, 15]

$$E_z(k,r) = -\frac{4ien_0 b(k)}{kr_{\rm b}^2}\left[1 - \frac{kr_{\rm b}}{\gamma}K_1\left(\frac{kr_{\rm b}}{\gamma}\right)I_0\left(\frac{kr}{\gamma}\right)\right] \tag{12}$$

for $r = \sqrt{x^2+y^2} \le r_{\rm b}$, where $r_{\rm b}$ is the beam radius for a circular cross section, K_1 and I_0 are the modified Bessel functions, and the velocity of the electrons is taken to be the speed

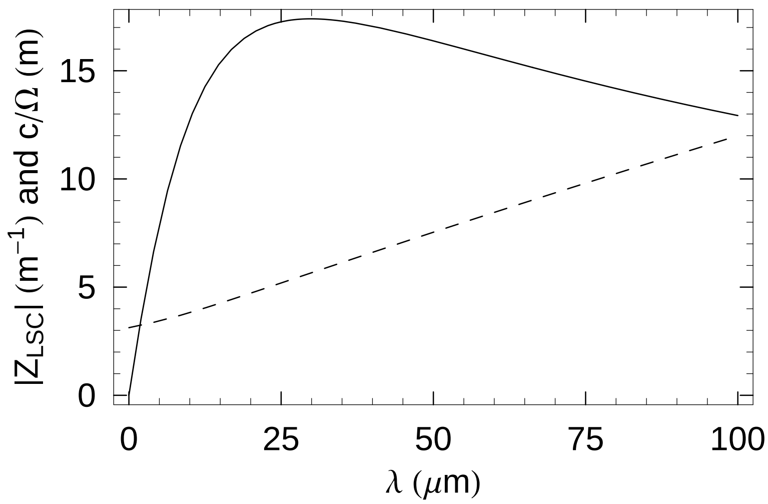

Figure 3: LSC impedance $Z_{\rm LSC}$ (solid line) and reduced space charge oscillation wavelength c/Ω (dashed line) as a function of the modulation wavelength for $\gamma = 130$, $r_{\rm b} = 580$ μm and $I_0 = 300$ A.

of light c. For simplicity, we average the electric field over the transverse cross section to obtain

$$\begin{aligned}\bar{E}_z(k) =& \frac{2}{r_{\rm b}^2}\int_0^{r_{\rm b}} dr r E_z(k,r) \\ =& -\frac{4ien_0 b(k;s)}{kr_{\rm b}^2}\left[1-\frac{kr_{\rm b}}{\gamma}K_1\left(\frac{kr_{\rm b}}{\gamma}\right)\right]R(k)\,,\end{aligned} \tag{13}$$

where the reduction factor R is typically slightly less than 1. The average LSC impedance per unit length is

$$\begin{aligned}Z_{\rm LSC}(k) =& \frac{4i}{kr_{\rm b}^2}\left[1-\frac{kr_{\rm b}}{\gamma}K_1\left(\frac{kr_{\rm b}}{\gamma}\right)\right]R(k) \\ \approx& \begin{cases}\frac{4i}{kr_{\rm b}^2}\,, & \frac{kr_{\rm b}}{\gamma}\gg 1\,, \\ \frac{ik}{\gamma^2}\left(1+2\ln\frac{\gamma}{r_{\rm b}k}\right)R(k)\,, & \frac{kr_{\rm b}}{\gamma}\ll 1\,.\end{cases}\end{aligned} \tag{14}$$

The free space approximation is satisfied when the beam pipe radius is much larger than the reduced modulation wavelength in the beam's rest frame $\gamma\lambda/(2\pi)$. For the SDL microbunching experiment, $\gamma \approx 130$, and the free space approximation is valid up to $\lambda \sim 100$ μm. Figure 3 shows this impedance using the SDL parameters.

In the zero-phasing accelerating cavities, the slip factor is simply $1/\gamma^2$ for a small energy deviation. A standard instability analysis [16] shows that the beam is stable for the LSC impedance with an oscillation frequency

$$\Omega = c\left[\frac{I_0}{\gamma^3 I_A}k|Z_{\rm LSC}(k)|\right]^{1/2}, \tag{15}$$

where $I_0 = n_0 ec$ is the peak electron current, and $I_A = 17045$ A is the Alfven current. In the limit that the transverse beam size is much larger than the reduced modulation wavelength in the beam's rest frame (i.e., $kr_{\rm b}/\gamma \gg 1$), Ω becomes the plasma frequency [15]. Fig. 3 shows the reduced space charge oscillation wavelength c/Ω as a function of the modulation wavelength for $I_0 = 300$ A after compression.

In this paper, we focus on the longitudinal beam dynamics in the SDL rf zero-phasing section. Since the upstream energy modulation can be effectively converted into current modulation through the chicane [12], we assume the beam has only the current modulation $b_0(k)$ and no energy modulation prior to the rf zero-phasing section (right after the bunch compressor). Thus, the bunching spectrum at the entrance of the spectrometer dipole after a drift distance ΔL is

$$b_{\rm d}(k) = b_0(k)\cos(\Omega\Delta L/c)\,. \tag{16}$$

The current modulation is converted into the energy modulation due to space charge oscillations, which is given by

$$\begin{aligned} p_{\rm d}(k) =& -\frac{I_0}{\gamma I_A}Z_{\rm LSC}(k)b_0(k)\sin(\Omega s/c)\frac{c}{\Omega} \\ =& -i\left[\frac{\gamma I_0}{I_A}\frac{|Z_{\rm LSC}(k)|}{k}\right]^{1/2}\sin\left(\frac{\Omega\Delta L}{c}\right)b_0(k)\,. \end{aligned} \tag{17}$$

Landau damping is ignored in the straight section because of the negligible path length difference for the very small energy spread and the emittance considered here. Note that the length of the SDL zero-phasing section, ΔL, is about 15 m. From Fig. 3, we see that $\Omega\Delta L/c \sim 1$ for a wide range of the modulation wavelength, so that the energy modulation is close to its maximum. Although we assume the average beam energy is constant in the zero-crossing accelerating section, the above analysis can be extended to other rf accelerating phases if the acceleration gradient is small compared to the beam energy divided by c/Ω.

4 Gain in horizontal modulation

As discussed in Sec. 2, the LSC induced energy modulation can be converted to an enhanced horizontal modulation in the spectrometer dipole. As a result, the horizontal modulation measured by the rf zero-phasing technique is much larger than the current modulation and may be quantified by a "gain" factor as

$$G_{\rm m} \equiv \left|\frac{a_{\rm m}(k_{\rm m})}{b_0(k)}\right|, \tag{18}$$

where the subscript m refers to the measurement screen. Inserting Eqs. (16) and (17) into Eq. (6), we obtain

$$G_{\mathrm{m}} = \left| \cos(\Omega\Delta L/c) - \frac{k}{h}\left[\frac{\gamma I_0}{I_A}\frac{|Z_{\mathrm{LSC}}(k)|}{k}\right]^{1/2}\sin(\Omega\Delta L/c)\right| \\ \times \exp\left[-\frac{k^2\sigma_\delta^2}{2h^2} - \frac{k^2(\sigma_x)_{\mathrm{m}}^2}{2h^2\eta_{\mathrm{m}}^2}\right] , \tag{19}$$

where the rms horizontal beam size at the screen is

$$(\sigma_x)_{\mathrm{m}} = (\sigma_x)_{\mathrm{d}}\left[\left(C_{\mathrm{m}} - \frac{\alpha_{\mathrm{d}} S_{\mathrm{m}}}{\beta_{\mathrm{d}}}\right)^2 + \frac{S_{\mathrm{m}}^2}{\beta_{\mathrm{d}}^2}\right] . \tag{20}$$

If the spectrometer dipole is a sector dipole with a bending radius ρ and a magnetic length L_{b}, the various lattice functions inside the dipole (for $s \leq L_{\mathrm{b}}$) are

$$C(s) = \cos\frac{s}{\rho}, \quad S(s) = \rho\sin\frac{s}{\rho}, \quad \eta(s) = \rho\left(1 - \cos\frac{s}{\rho}\right) .$$

For a measurement screen located at a distance L_{s} behind the dipole, the final lattice functions at the screen are

$$C_{\mathrm{m}} = \cos\frac{L_{\mathrm{b}}}{\rho} - \frac{L_{\mathrm{s}}}{\rho}\sin\frac{L_{\mathrm{b}}}{\rho}, \quad S_{\mathrm{m}} = \rho\sin\frac{L_{\mathrm{b}}}{\rho} + L_{\mathrm{s}}\cos\frac{L_{\mathrm{b}}}{\rho}, \\ \eta_{\mathrm{m}} = \rho\left(1 - \cos\frac{L_{\mathrm{b}}}{\rho}\right) + L_{\mathrm{s}}\sin\frac{L_{\mathrm{b}}}{\rho} . \tag{21}$$

Equation (19) gives the apparent "gain" of the horizontal density modulation to the longitudinal density modulation as a function of the modulation wavelength λ. We apply this formula to study the SDL microbunching experiment with the typical parameters listed in Table 1. As shown in Fig. 4, the gain is much larger than 1 for a wide range of modulation wavelengths above the resolution limit (except for wavelengths corresponding to $c/\Omega = 2\Delta L/n$ for $n = 1, 2, 3, ...$), indicating that the horizontal spectrum is dominated by effects of the energy modulation. When $G_{\mathrm{m}} \gg 1$ and $|p_{\mathrm{d}}(k)| \ll h\lambda/(2\pi)$, we have from Eq. (6)

$$p_{\mathrm{d}}(k) \approx i\frac{h}{k}a_{\mathrm{m}}(k_{\mathrm{m}}) \tag{22}$$

above the resolution limit. For the energy modulation comparable to the energy chirp over the modulation wavelength, other methods can be used to obtain p_{d} [17]. Therefore, the rf zero-phasing technique can be used to extract the beam energy modulation instead of the current modulation.

Table 1: Typical parameters for the SDL microbunching experiments.

Parameter	Symbol	Value
beam energy	E	65 MeV
compressed peak current	I_0	300 A
normalized emittance	$\gamma\varepsilon_x$	2.5 μm
average beam radius	$r_{\rm b}$	580 μm
beta at dipole	$\beta_{\rm d}$	8.5 m
alpha at dipole	$\alpha_{\rm d}$	1.8
incoherent energy spread	σ_δ	1×10^{-4}
chirp	h	± 50 m^{-1}
zero-phasing linac length	ΔL	15 m
dipole bending radius	ρ	0.79 m
dipole magnetic length	$L_{\rm s}$	1m
total dipole R_{56}	R_{56}	-24.5 cm
distance from dipole to screen	$L_{\rm s}$	0.31 m

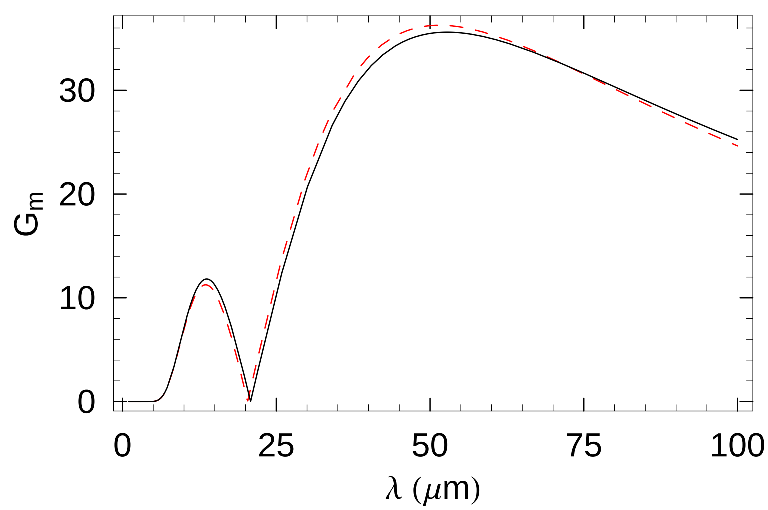

Figure 4: (Color) Gain of the horizontal density modulation relative to the current modulation as a function of the modulation wavelength at the entrance of the dipole for the negative chirp (solid line) and the positive chirp (dashed line).

5 Conclusion

In this paper, we study the rf zero-phasing technique for a general beam distribution and show that the measured horizontal profile is very sensitive to the beam energy modulation. For high-brightness electron beams, the energy modulation can be induced by the longitudinal space charge force in the accelerator and can significantly distort the horizontal profile. This analysis is applied to the SDL microbunching experiment and provides a qualitative explanation for the observed structures [18]. Beam dynamics studies in the SDL accelerator are planned to address sources of the initial modulation and effects of acceleration and compression.

Acknowledgments

We wish to thank A. Chao, D. Dowell, P. Emma, and C. Limborg for useful discussions.

References

[1] See, for example, P. Krejcik, "short bunch beam diagnostics," SLAC-PUB-9527, 2002.

[2] D.X. Wang, G.A. Krafft, and C.K. Sinclair, Phys. Rev. E **57**, 2283 (1998).

[3] W.S. Graves *et al.*, in *Proc. of the 2001 Particle Accelerator Conference*, 2224 (2001); *ibid*, 2860 (2001).

[4] S. Heifets, G. Stupakov, S. Krinsky, Phys. Rev. ST Accel. Beams **5**, 064401 (2002).

[5] Z. Huang, K.-J. Kim, Phys. Rev. ST Accel. Beams **5**, 074401 (2002).

[6] H. Loos *et al.*, in *Proc. of the 2002 European Particle Accelerator Conference*, 814 (2002).

[7] H.H. Braun *et al.*, Phys. Rev. ST Accel. Beams **3**, 124402 (2000).

[8] Ph. Piot *et al.*, in *Proc. of the 2000 European Particle Accelerator Conference*, 1546 (2000).

[9] M. Huning, Ph. Piot, H. Schlarb, Nucl. Instrum. Methods Phys. Res., Sect. A **475**, 348 (2001).

[10] E.L. Saldin, E.A. Schneidmiller, M.V. Yurkov, Nucl. Instrum. Methods Phys. Res., Sect. A **490** 1 (2002).

[11] Z. Huang *et al.*, in *Proc. of the 2003 Particle Accelerator Conference*, 2003.

[12] E.L. Saldin, E.A. Schneidmiller, M.V. Yurkov, "Longitudinal Space Charge Driven Microbunching Instability in TTF2 Linac," TESLA-FEL-2003-02, 2003.

[13] Collective effects such as coherent synchrotron radiation in the spectrometer dipole is usually small due to Landau damping arising from beam emittance and energy spread.

[14] J. Rosenzweig *et al.*, “Space-charge oscillations in a self-modulated electron beam in multi-undulator free-electron lasers,” DESY-TESLA-FEL-96-15, 1996.

[15] M. Chodorow and C. Susskind, *Fundamentals of Microwave Electronics* (McGraw-Hill, New York, 1961).

[16] A. Chao, *Physics of Collective Beam Instabilities in High Energy Accelerators* (Wiley, New York, 1993).

[17] T. Shaftan and L.-H. Yu, “Analysis of space charge driven modulation in electron bunch energy spectra,” to be published.

[18] T. Shaftan *et al.*, in *Proc. of the 2003 Particle Accelerator Conference*, 2003.